British Journal of Pharmacology (2006) 149, 600–607
 0007–1188/06 $30.00
www.brjpharmacol.org

RESEARCH PAPER

Inhibition by α-Tetrahydrodeoxycorticosterone (THDOC) of Pre-Sympathetic Parvocellular Neurones in the Paraventricular Nucleus of Rat Hypothalamus

MD Womack[1], S Pyner[2] and R Barrett-Jolley[1]

[1]*Department of Veterinary Preclinical Sciences, University of Liverpool, Liverpool, UK and* [2]*School of Biological & Biomedical Sciences, Science Laboratories, University of Durham, Durham, UK*

Background and Purpose: α-tetrahydrodeoxycorticosterone (THDOC) is an endogenous neuroactive steroid which increases in plasma and brain concentration during stress. It has both positive and negative modulatory effects on GABA activated $GABA_A$ currents, dependent upon the dose. We investigated the effects of THDOC on spinally-projecting ''pre-sympathetic'' neurones in the parvocellular subnucleus of the hypothalamic paraventricular nucleus (PVN), to determine whether it activates or inhibits these neurones, and by what mechanism.
Experimental Approach: Rat spinally-projecting (parvocellular) PVN neurones were identified by retrograde labelling and the action of THDOC investigated with three modes of patch-clamp: cell-attached action current, whole-cell voltage-clamp and cell-attached single-channel recording.
Key Results: In cell-attached patch mode, parvocellular neurones fired action potentials spontaneously with an average frequency of 3.6 ± 1.1Hz. Bath application of THDOC reduced this with an EC_{50} of 67nM (95% confidence limits: 54 to 84nM), Hill coefficient 0.8 ± 0.04, $n = 5$. In whole-cell patch-clamp mode, pressure ejection of GABA evoked inward currents. These were clearly $GABA_A$ currents, since they were inhibited by the $GABA_A$ receptor antagonist bicuculline, and reversed near the chloride equilibrium potential. THDOC significantly potentiated $GABA_A$ currents (1μM THDOC: 148 ± 15% of control, $n = 5$, $p \leq 0.05$, ANOVA). Single-channel analysis showed no differences in conductance or corrected mean open times in the presence of 1μM THDOC.
Conclusions and Implications: THDOC inhibited parvocellular neuronal activity without showing any evidence of the bidirectional activity demonstrated previously with cultured hypothalamic neurones. Our data are consistent with the hypothesis that THDOC acts by potentiating the post-synaptic activity of endogenously released GABA.
British Journal of Pharmacology (2006) **149**, 600–607. doi:10.1038/sj.bjp.0706911; published online 25 September 2006

Keywords: THDOC; GABA; spinally projecting neurones; sympathetic; cardiovascular control

Abbreviations: ACSF, artificial cerebrospinal fluid; CL, confidence limits; E_{Cl}, equilibrium potential for chloride ions; P_o, channel open probability; PVN, paraventricular nucleus; THDOC, α-tetrahydrodeoxycorticosterone

Introduction

The paraventricular nucleus (PVN) of the hypothalamus is central to integration of the physiological stress response. It consists of neurones which control the hypothalamic–pituitary axis (Buckingham, 1996; Sawchenko *et al*., 1996), and neurones which project to sympathetic centres in the spinal cord (Swanson and Kuypers, 1980a, b; Swanson *et al*., 1986; Rho and Swanson, 1989; Hosoya *et al*., 1991) and rostral ventrolateral medulla (Shafton *et al*., 1998; Pyner and Coote, 2000) increasing both heart rate and blood pressure (Coote, 1995; Badoer, 1996; Akine *et al*., 2003). These spinally projecting, parvocellular neurones express $GABA_A$ receptors (Cui *et al*., 2001; Li *et al*., 2002), and are believed to be tonically inhibited by endogenous GABA, as studies have shown that intra-paraventricular injection of a $GABA_A$ antagonist (bicuculline) also increases sympathetic output, blood pressure and heart rate (Martin *et al*., 1991; Martin and Haywood, 1993; Schlenker *et al*., 2001). However, the primary physiological role of these paraventricular 'pre-sympathetic' neurones remains controversial. Although some reports suggest PVN involvement in the cardiovascular

Correspondence: Dr R Barrett-Jolley, Department of Veterinary Preclinical Sciences, University of Liverpool, Liverpool L69 7ZJ, UK.
E-mail: RBJ@Liverpool.ac.uk
Received 1 August 2006; accepted 21 August 2006; published online 25 September 2006

response to stress (Duan *et al*., 1997), inhibition of neuronal activity by PVN injection of muscimol (a $GABA_A$ selective agonist) does not appear to prevent the response to stress (Stotz-Potter *et al*., 1996a, b).

During acute stress, when sympathetic activity is known to be increased, there is also an elevation in hypothalamic concentrations of neuroactive steroids (Purdy *et al*., 1991; Paul and Purdy, 1992). Many of these neuroactive steroids are positive allosteric modulators of $GABA_A$ receptor channels (Majewska *et al*., 1985), although one such neuroactive steroid, pregnenolone, has been shown to be an inhibitor of $GABA_A$ function (Majewska *et al*., 1988). Another neuroactive steroid, α-tetrahydrodeoxycorticosterone (THDOC), has been reported to enhance, inhibit or be inactive on $GABA_A$ receptor currents, depending on the dose (Wetzel *et al*., 1999), the receptor subunit composition (Zhu *et al*., 1996) or the type of neurone under study (Cooper *et al*., 1999). Without further experimental evidence, it is therefore impossible to predict whether stress-induced elevations of THDOC would be excitatory, inhibitory or inactive on parvocellular neurones. This is important because the activity of spinally projecting neurones could potentially contribute to the increase in sympathetic activity seen during a number of divergent stress stimuli. In this study, we have addressed this question by recording from parvocellular neurones in hypothalamic slices, and report the effects of THDOC both on the frequency of spontaneously generated action currents and whole-cell and unitary $GABA_A$ currents of parvocellular neurones.

Methods

Animals

In this work, a total of 28 Wistar rats of either sex (50–80 g body weight) were used. Animals were maintained and all experiments were carried out humanely, in accordance with UK Home Office regulations under Project Licence 40/2211.6.

Retrograde labelling of parvocellular PVN neurones

Electrophysiological experiments were conducted on parvocellular PVN neurones identified anatomically (Paxinos and Watson, 1986) and by either morphology (Rho and Swanson, 1989) and/or by retrograde labelling (Barrett-Jolley *et al*., 2000).

Retrograde labelling methods were similar to those described previously (Barrett-Jolley *et al*., 2000); PVN spinally projecting neurones were labelled by injection of a fluorescent red retrograde tracer (1,1′-dioctadecyl-3,3,3′,3′-tetramethylindocarbocyanine perchlorate, DiI, Molecular Probes, Paisley, UK) into the spinal cord intermediolateralis (T2–T4) of 3–4-week-old rats under general anaesthesia (intraperitoneal injection of metatomidine ($0.6\,mg\,kg^{-1}$) and ketamine ($30\,mg\,kg^{-1}$)). The vertebral column was stabilized with a stereotactic clamp and a glass micropipette positioned vertically, with the tip 500 μm below the surface of the lateral sulcus. Approximately, 100 nl DiI (0.4%) was then injected into the cord. The pipette was left in position for 5 min following injection to allow the DiI to fully diffuse throughout the injection site.

Hypothalamic slice recording

Slices of PVN were prepared for *in vitro* recording by standard brain slice methods; briefly, rats were deeply anaesthetized with ether and then killed by decapitation. The brain was removed to iced artificial cerebrospinal fluid (ACSF). The general area of the hypothalamus was blocked and glued in the chamber of a Campden Instruments Vibroslice (Loughborough, UK). The chamber was maintained at 0–4°C by frequent addition of ice to the outer cooling chamber. Coronal slices, approximately 250 μm, were cut and removed to a multiwell culture dish containing normal ACSF. The culture dish was incubated at 35–37°C and bubbled with 95% O_2/5% CO_2, for at least 1 h before recording.

In all brain slice experiments, slices were perfused at 1 bath volume/min with a modified ACSF (equilibrated with 95% O_2/5% CO_2) (see Solutions) and maintained at 34–36°C. Neurones were visualized with a Nikon E600FN Eclipse upright microscope equipped with near infrared DIC optics. Spinally projecting (retrogradely labelled) neurones could be identified by viewing through an appropriate filter block (Nikon G2A: Ex510-560, DM575, BA590 nm). In all experiments, patch pipettes were fabricated from thick-walled borosilicate glass (Harvard's 'Clark GC150F') using either a Brown-Flaming MP P-80 horizontal puller (Sutter Instrument Co., Novato, CA, USA) or a vertical Narishige two-stage patch pipette puller (PP-830, purchased from Digitimer, UK). When filled, pipettes had resistances of approximately 5 MΩ. Data were recorded with an Axon Axopatch 200B amplifier and low pass filtered at between 0.1 and 10 kHz as appropriate. In the case of action current measurement, data were additionally high passed filtered at 0.1 Hz, a level of adenylyl cyclase coupling which has no effect on the action current waveform. Analysis was performed with a range of non-commercial PC programmes (see Software).

Action current frequency experiments

Action currents were measured from retrogradely labelled spinally projecting neurones by means of the cell-attached patch technique following the methods of Fenwick *et al*. (1982). These methods were also used previously by Costantin and Charles (2001), Fischmeister *et al*. (1984) and ourselves (Zaki and Barrett-Jolley, 2002). A full explanation of this technique is given by Fenwick *et al*. (1982). Briefly, after formation of a tight seal (cell-attached patch), the command voltage was permanently set to 0 mV. Measured current is then the sum of the resistive and capacitance currents flowing between the cell interior and the patch pipette. It is theoretically possible to derive absolute membrane potential values for the underlying action potential (Fenwick *et al*., 1982); however, this requires very accurate discrimination between membrane patch resistance and seal resistance. In the experiments reported in this paper, action currents are used simply to allow precise measurement of underlying action potential frequency, without penetration of the cell or rupture of the cell

membrane. Importantly, this method does not disturb the intracellular environment of the target neurone.

Action of THDOC was assessed following 4–5 min of exposure, approximately 5 min stretches of action current recordings were then analysed under control and test conditions. Neurones with initial action current frequency of above 0.05 Hz were accepted for study. Data are expressed as relative action current frequency before and during treatment with THDOC and fit with the following equation (Black and Shankley, 1985):

$$R = 1 - \frac{[THDOC]^{h}}{[THDOC]^{h} + 10^{\log(EC_{50}).n_{h}}}. \quad (1)$$

where R is the relative frequency in the presence (*THDOC*) molar THDOC, EC_{50} is the midpoint of the logistic equation and n_h is the Hill coefficient. Error-weighted curve fitting was performed with SigmaPlot (see Software) and appropriate logarithmic transformations are presented in the text.

Whole-cell voltage-clamp

Whole-cell GABA currents were recorded from parvocellular neurones under similar conditions to those of the action current recording experiments (above); however, cells were held at −60 mV and we used modified, low chloride ACSF flow solution (see Solutions). GABA was applied by pressure ejection using a Picospritzer (General Valve Corporation, Fairfield, NJ, USA) connected to a puffer pipette. The puffer pipette had a tip opening of approximately 5 μm, was filled with GABA 300 μM and positioned approximately 100 μm from the subject neurone. GABA (300 μM) was then applied in a brief (usually 500 ms) pulse at 90 s intervals.

Single-channel analysis

For single-channel analysis, contiguous stretches of channel activity were recorded in cell-attached patch mode (holding potential −100 mV). The recording pipette contained an extracellular solution (see Solutions) and 100 μM GABA. Where currents were recorded in the presence of THDOC, 1 μM THDOC was included, along with the GABA in the patch pipette. For measurement of both single-channel amplitude and kinetics, stretches of recording with more than one active channel were excluded. Channel activity was filtered at 1 kHz and sampled at 100 μs, and analysis performed with a Windows PC programme (see 'Software'). Events were detected on the basis of 50% event detection and log-binned at 25 bins per $\log_{10}$ unit (Sigworth and Sine, 1987). Histograms present these data with a root frequency X-axis. We imposed a minimum resolution of 100 μs and fit data with the following probability density function, by maximum likelihood:

$$f(t) = \sum_{j=1}^{m} (a_j/\tau_j) \exp(-t/\tau_j). \quad (2)$$

where a_j is the relative area of component j, τ_j is time constant of exponential component j and m is the number of components. Openings interrupted by undetectably brief closures distort calculation of open times. This was corrected for by multiplying the mean open time by the proportion of detected closed times (given by the integral of the closed time fit, between the minimum time and infinity) to give a 'corrected mean open time' (cmot).

We defined bursts to be groups of openings separated by closures shorter than a critical time (t_{crit}), calculated by defining the shortest components of closed time distributions as gaps within bursts and matching the proportion of short closings misclassified as long to the long closings misclassified as short (Colquhoun and Sakmann, 1985).

It is assumed that a whole-cell ion channel current can be compared to single-channel current by the following equation:

$$I = n.P_o.i. \quad (3)$$

where I is the macroscopic current, n is the number of channels, channel open probability (P_o) is the probability of a channel being open and i is the unitary amplitude. For any given holding potential, and with the same recording conditions, i is proportional to unitary conductance. In this study, we calculate mean open times, rather than P_o specifically.

Software

Data were acquired through an Axon DigiData 1200 interface card driven by either the analysis and acquisition programme (called 'WCP', by John Dempster, Strathclyde University) or the 'Axgox' and 'Tracwin' programmes (Noel Davies, Leicester University) as appropriate. Whole-cell analysis was performed with 'WCP' and single-channel analysis was performed with 'Tracwin'. Further details of software are available on our website (http://pcwww.liv.ac.uk/~rbj/RBJ/software.htm).

Solutions

Action current experiments used a standard high-sodium ACSF extracellular solution (mM): 125 NaCl, 2.5 KCl, 26 $NaHCO_3$, 10 glucose, 1.25 NaH_2PO_4, 1.2 $MgCl_2$ (with either 2.5 or 0.5 'low calcium' $CaCl_2$) (pH 7.4) when equilibrated with 95% O_2/5% CO_2. The pipette solution for all experiments was (mM) 150 KCl_2, 1.4 $MgCl_2$, 10 EGTA, 10 HEPES; pH adjusted to 7.2 with potassium hydroxide. All GABA currents (outside-out patch and whole-cell) were recorded using a low-sodium HEPES-buffered extracellular (flow) solution (mM): Na_2SO_4 65, $NaCHO_3$ 26, NaCl 25, glucose 10, $CaCl_2$ 4, KCl 1.9, $MgSO_4$ 1.3, KH_2PO_4 1.2 and gassed with 95% O_2/5% CO_2. THDOC was dissolved in dimethyl sulphoxide (DMSO. as 100 mM stocks). The final concentration of DMSO never exceeded 1:1000, at which level it is inactive in the assays reported in this paper.

Statistical analysis

Data are presented as mean (95% confidence limit (CL)) or mean ± s.e., as appropriate. n refers to the number of experiments. '$P \leqslant x$' values are derived from ANOVA tests

(with Bonferroni multiple comparison correction, where appropriate and stated), calculated with StatsDirect (see Software). A probability of less than 0.05 is defined as statistically significant.

Materials

All drugs and chemicals were supplied by the Sigma-Aldrich Company Ltd, Poole, Dorset (UK).

Results

Action current frequency

To assess whether spinally projecting parvocellular neurones were activated, or inhibited by THDOC in the normal physiological range, we began by measuring spontaneous action current activity before and during bath application of THDOC. As shown in Figure 1a, we found THDOC at a concentration of 1 μM to reduce markedly the spontaneous action current frequency and by extending the concentration range of THDOC from 10 nM to 10 μM (Figure 1b), we calculated that THDOC inhibited spontaneous action current frequency with an EC_{50} value of 67 nM (95% CL: 54–84 nM; Hill coefficient 0.8 ± 0.04: $n = 5$).

This inhibitory effect of THDOC could be mediated via modulation of $GABA_A$ receptors, as parvocellular neurones are powerfully inhibited by GABA (Zaki and Barrett-Jolley, 2002). We therefore assessed the effects of the $GABA_A$ antagonist, bicuculline, applying 10 μM bicuculline to spontaneously firing parvocellular neurones and then adding 1 μM THDOC (Figure 1c). Under these conditions, THDOC no longer caused a significant reduction of action current frequency (Figure 1d).

Whole-cell patch-clamp

Next, we made whole-cell patch-clamp recordings from parvocellular neurones and applied GABA to these neurones, directly from a pressure ejection pipette. This elicited large inward currents in the recorded parvocellular neurone. These currents reversed near the calculated chloride equilibrium potential (Figure 2a) and were inhibited by the $GABA_A$ antagonist bicuculline (Figure 2b).

When THDOC was added to the bath flow solution at a concentration of 1 μM, the amplitude of these $GABA_A$ currents was increased in a reversible manner by about 50% (Figure 2b, c). Wetzel *et al*. (1999) observed that at low concentrations, THDOC had an inhibitory action. We therefore repeated these experiments at concentrations as

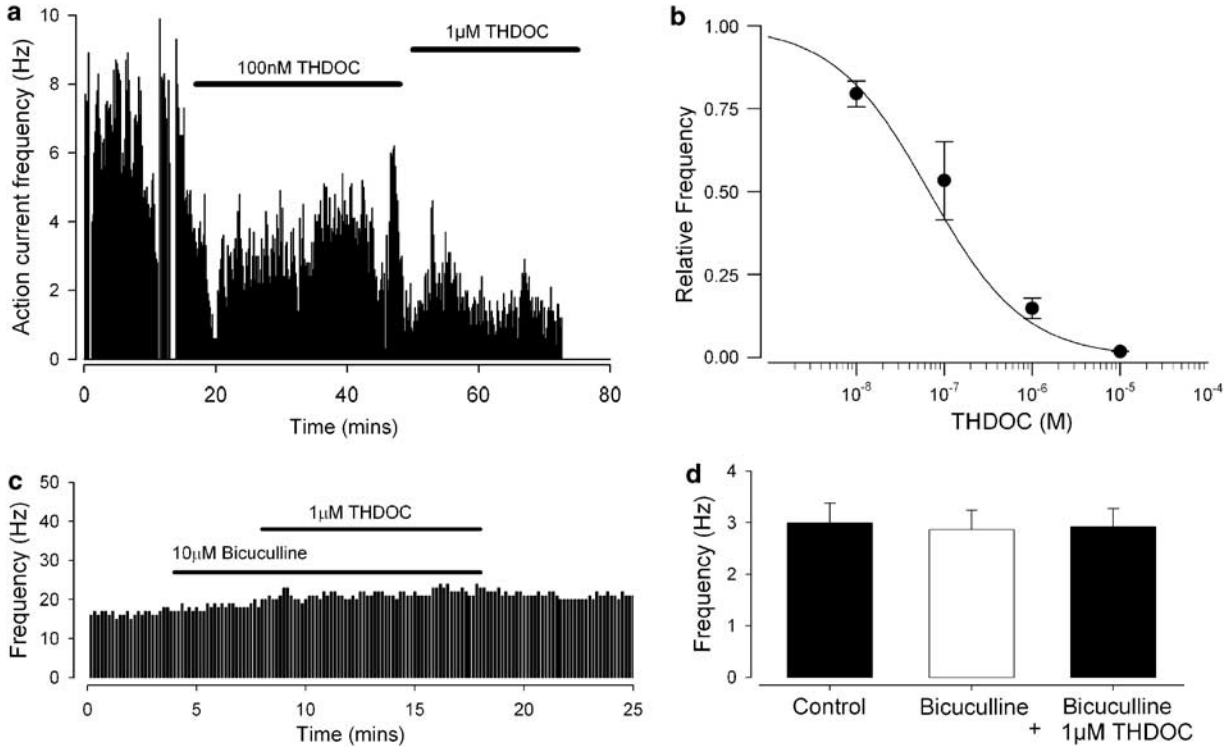

Figure 1 THDOC decreases action current frequency in spinally projecting parvocellular neurones. (**a**) Action currents recorded in retrogradely spinally projecting parvocellular neurones in cell-attached patch mode; frequency (*Y*-axis) is plotted against time (*X*-axis). THDOC (100 nM and 1 μM) was added where indicated by the bars. (**b**) Summary of five experiments as illustrated in (**a**), but with a range of concentrations. The smooth line represents an error-weighted fit to the mean data (Equation 1); best fit parameters were EC_{50} 67 nM with 95% CLs of 54 and 84 nM, Hill coefficient 0.8 ± 0.04, $n = 5$. *X*-axis is a log scale. (**c**) Representative figure showing the lack of effect of 1 μM THDOC when applied in the presence of the $GABA_A$ antagonist, bicuculline. (**d**) Mean data from seven experiments, as illustrated in (**c**) bicuculline concentration 10 μM. Action current frequency in the presence of THDOC and bicuculline was not significantly different from that in either control or 10 μM bicuculline (ANOVA, $n = 7$).

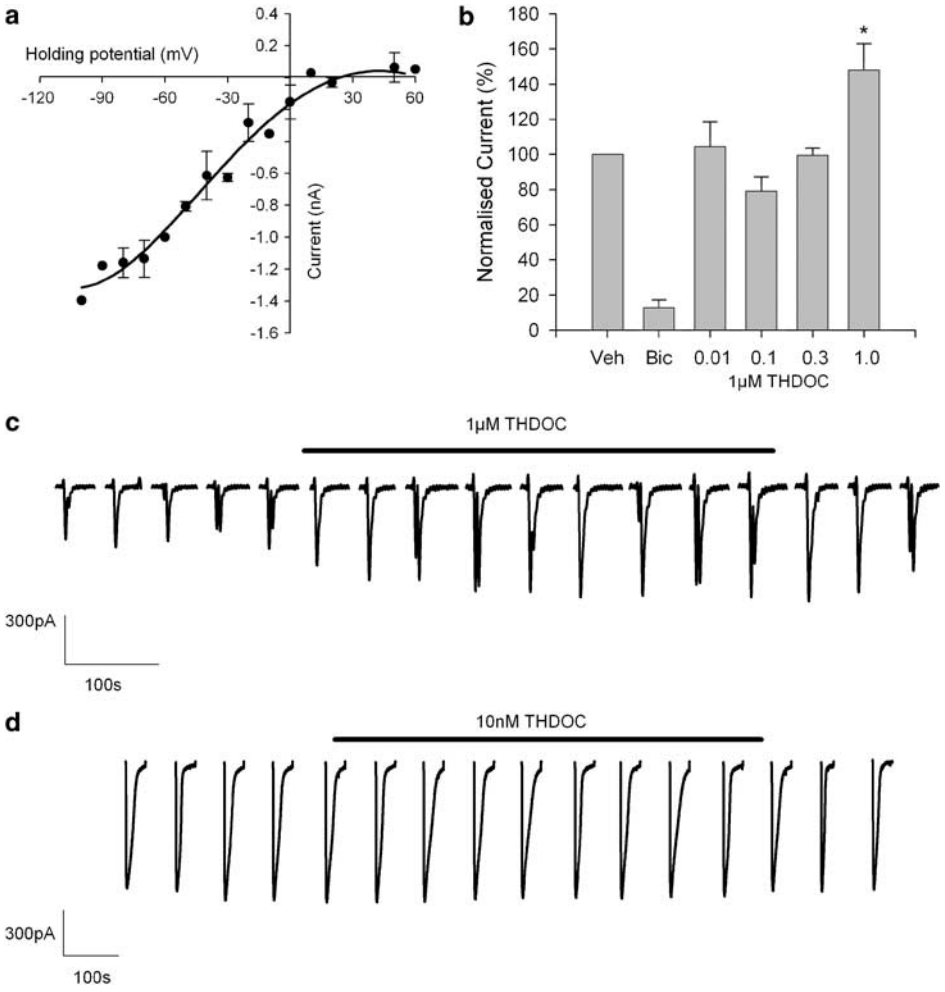

Figure 2 THDOC (1 μM) increases GABA whole-cell currents. (**a**) Current–voltage curve for GABA whole-cell currents; a smooth line is drawn through the points ($n=5$). (**b**) Summary of vehicle (veh), bicuculline (10 μM, bic) and THDOC (concentrations given in μM) effects on GABA (300 μM) whole-cell currents. The *Y*-axis is percentage normalized current in test compared to control. Vehicle $n=18$, bicuculline $n=5$, THDOC (μM): (0.01) $n=3$, (0.1) $n=4$, (0.3) $n=3$, (1) $n=5$. *$P<0.05$ ANOVA. (**c**) GABA whole-cell currents in the presence and absence of 1 μM THDOC (THDOC bath application indicated by the bar), GABA (300 μM) was applied by pressure ejection. (**d**) A similar experiment to that shown in (**c**), but with 10 nM THDOC.

low as 10 nM (Figure 2b, d), but failed to detect any inhibition by THDOC at these concentrations.

Single-channel kinetics

To identify a possible mechanism by which THDOC increased whole-cell $GABA_A$ currents, we investigated changes in single-channel behaviour using cell-attached recording from parvocellular neurones. Figure 3a shows $GABA_A$ single-channel activity in a cell-attached patch recording from a parvocellular PVN neurone in the presence and absence of 1 μM THDOC. We began by investigating whether $GABA_A$ channel conductance is altered by THDOC. We calculated chord conductance between the holding potential of -100 mV holding potential and the reversal potential (E_{Cl}) with and without 1 μM THDOC. Conductances were both in the range of 10–12 pS, and there was no significant difference between events measured in the presence of 100 μM GABA or those measured in the presence of 100 μM GABA with 1 μM THDOC (Figure 3b). As there is no change in $GABA_A$ channel conductance ('*i*', Equation 3), but an increase of whole-cell $GABA_A$ current, logic dictates there is likely to be a change in either the number of active channels ('*n*', Equation 3), or of the channel kinetic properties (i.e., 'P_o', Equation 3). We therefore undertook kinetic analysis of $GABA_A$ channel activity in the presence of THDOC, again in cell-attached patch mode. We recorded channel activity at $+20$ mV (holding potential) with 100 μM GABA and the presence or absence of 1 μM THDOC. Interestingly, there was no significant difference in burst length, corrected mean open time or open time within bursts compared to those in the presence of 1 μM THDOC (Figure 3c, d).

Discussion

In this work, we show the neuroactive steroid THDOC to be a potent inhibitor of the neuronal activity of spinally projecting parvocellular neurones in the rat PVN. We show this

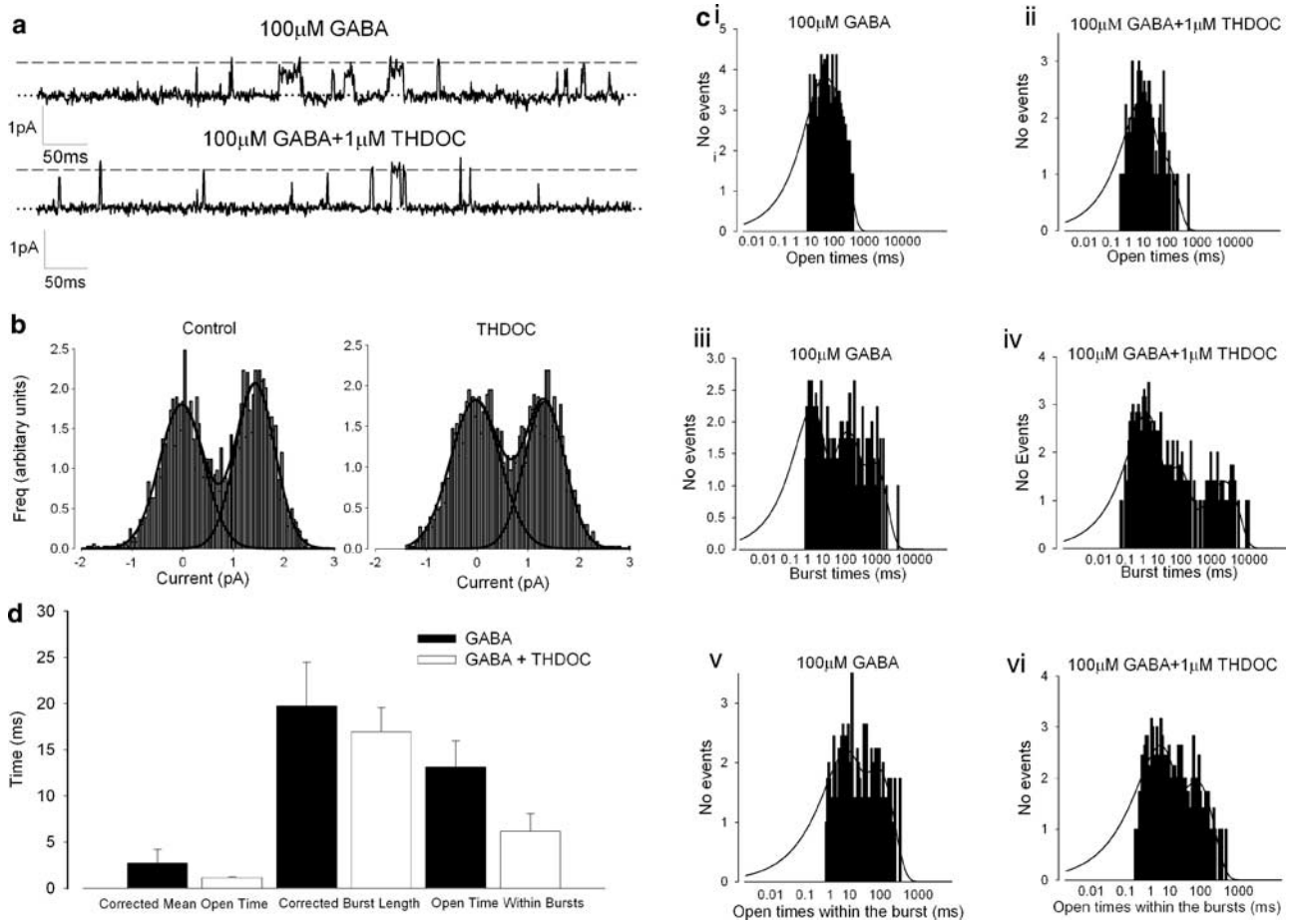

Figure 3 Single-channel analysis of THDOC effect. (**a**) Recording from GABA-activated single channels (cell-attached patch mode) from parvocellular neurone membrane. Upper trace GABA alone (100 μM), lower trace in the presence of 100 μM GABA + 1 μM THDOC. The dotted line represents the zero current level (channels closed) and channel openings are seen as upward deflections. The approximate unitary current level is shown by the dashed line. (**b**) All-point amplitude histograms for GABA alone (100 μM) on the left, and for 100 μM GABA + 1 μM THDOC on the right. At −100 mV, chord conductances were not significantly different (12.2 ± 0.6 and 10.9 ± 0.5 pS, $n = 11$; two-way ANOVA). (**c**) Dwell–time histograms from kinetic analysis of GABA channels in the presence of 100 μM GABA (**c** i, **c** iii and **c** v) or 100 μM GABA + 1 μM THDOC (**c** ii, **c** iv and **c** vi). Openings (**c** i and **c** ii), burst length (**c** iii and **c** iv) and open-time within bursts (**c** v and **c** vi). (**d**) Corrected mean open time, burst lengths and open times within bursts with 100 μm GABA (filled bars) or 100 μm GABA + 1 μM THDOC (open bars). $n = 4$ for GABA alone and $n = 6$ for GABA + THDOC experiments ($P > 0.05$, ANOVA with Bonferroni multiple comparison correction in all cases).

reduction in action potential firing frequency to result from a positive modulation of $GABA_A$ currents. We saw no evidence of the low-dose $GABA_A$ inhibition previously reported for THDOC on dissociated hypothalamic neurones (Wetzel *et al*., 1999).

Neuroactive steroid actions on $GABA_A$ receptors

A number of steroids have been reported to modulate the activity of GABA, the primary inhibitory neurotransmitter in the vertebrate brain. Naturally, this modulation of GABA activity leads to a modulation of neuronal activity. These neuroactive steroids have been shown to act either as antagonists of the binding of GABA to its receptor (e.g., pregnenolone sulphate, Majewska *et al*., 1988; Mienville and Vicini, 1989), or as positive allosteric modulators (e.g., allopregnanolone, Majewska *et al*., 1986). The nature of the allosteric modulation itself has been the subject of study by a number of groups and two conflicting mechanisms have been proposed. The first involves steroid binding to the $GABA_A$ receptor, and an allosteric action analogous to that for classic $GABA_A$ modulators such as benzodiazepines (Harrison *et al*., 1987). The alternative mechanism involves phosphorylation-dependent coupling between a proposed steroid binding site and the $GABA_A$ receptor channel complex (Fancsik *et al*., 2000). In either case, it is now well established that neurosteroid actions are often dependent on the subunit composition of the $GABA_A$ receptor (Maitra and Reynolds, 1999; Bianchi and Macdonald, 2001). The neuroactive steroid THDOC itself is remarkable, because it has been observed, that in some preparations, THDOC turns from an inhibitor of GABA currents to an activator as concentration increases (Wetzel *et al*., 1999). Thus, THDOC could potentially have no effect, an inhibitory or an excitatory activity on any specific population of neurones, depending on nature of the particular $GABA_A$ receptors and the local concentration of steroid.

Effect of THDOC on parvocellular action current frequency
Spinally projecting parvocellular neurones are believed to be tonically inhibited by local GABAergic input within the PVN (Martin *et al*., 1991; Martin and Haywood, 1993; Schlenker *et al*., 2001), and any inhibition of this tonic GABA activity by steroids would be expected to increase sympathetic outflow. It was therefore important to determine whether parvocellular neurones were activated or inhibited by concentrations of THDOC that would be expected at rest and during stress.

Concentrations of neuroactive steroids have been studied in a number of brain regions both in the presence and absence of stress. Concentrations increase in plasma, hypothalamus and cortical tissue during stress by some 5- to 20-fold (Purdy *et al*., 1991). Exact local concentrations of THDOC in the biophase of the hypothalamic $GABA_A$ receptor are unknown; however, some authors estimate that the maximum concentration of THDOC seen during stress would be in the order of 20 nM (Wetzel *et al*., 1999; Reddy and Rogawski, 2002). We found parvocellular action current frequency to be decreased by THDOC with an EC_{50} of approximately 70 nM. Assuming that, *in vivo* THDOC acts with a similar potency, and that, during stress, THDOC concentrations rise to approximately 20 nM (Wetzel *et al*., 1999; Reddy and Rogawski, 2002), this would result in a small decrease in tonic action potential frequency of spinally projecting PVN neurones.

Effect of THDOC on parvocellular $GABA_A$ current amplitude
Confirmation that the action of THDOC involves $GABA_A$ receptors comes from our observation that THDOC did not change action current frequency when applied in the presence of the selective $GABA_A$ antagonist bicuculline. Our results with spontaneous action current frequency would be consistent with a positive modulation of parvocellular neurone $GABA_A$ receptors by THDOC. To confirm this, we studied the action of THDOC with whole-cell patch-clamp. Our whole-cell data largely support this hypothesis; 1 μM THDOC increases $GABA_A$ currents by approximately 50%. However, unlike Wetzel *et al*. (1999), we saw no $GABA_A$ inhibition with low concentrations of THDOC (10 nM, for example). The most obvious explanation for why we do not see these bidirectional effects (Wetzel *et al*., 1999) is that the phenotype of the target neurones are different. Wetzel *et al*. (1999) investigated the interaction of THDOC on cultured hypothalamic neurones, whereas we based our study on spinally projecting neurones of the PVN, in slices of tissue. For example, there will undoubtedly be differences in the subtypes of $GABA_A$ receptors expressed. Parvocellular PVN neurones express principally α_2- (rather than α_1-) subunits (Fritschy and Mohler, 1995; Barrett-Jolley and Pyner, 2003), but there is little available data on the remaining make up of their $GABA_A$ receptors. The subunit composition of the $GABA_A$ receptors involved in the work by Wetzel *et al*. (1999) is unknown. Another possible explanation for the major differences between the effects of THDOC on cultured hypothalamic neurones (Wetzel *et al*., 1999) and our preparation of parvocellular neurones, in slice, is that THDOC is a highly lipophilic species and will partition into the cell membranes of surrounding neurophil. This could lead to important differences in biophase concentrations of THDOC in the two different systems.

Mechanism of action of THDOC: single-channel study
At the single-channel level, we saw no effects of THDOC. Kinetic analysis showed no significant change in $GABA_A$ cmot, closed times, burst length or open times within the burst in the presence of THDOC that would account for the increase in whole-cell current. In some preparations, benzodiazepines have been shown to increase $GABA_A$ channel conductance (Eghbali *et al*., 1997), and so this seemed a plausible mechanism for the action of THDOC. However, we also saw no changes in $GABA_A$ unitary conductance with addition of THDOC. From the canonical relation between whole-cell and unitary-current amplitude (Equation 3), the possibility remains, therefore, that THDOC increases the availability of $GABA_A$ channels. Interestingly, this is the mechanism proposed for the regulation of recombinant $GABA_A$ receptors by protein kinase C *in vitro* (Connolly *et al*., 1999).

In conclusion, we show for the first time, the effect of THDOC on neurones thought to be important for integration of the stress response, namely, spinally projecting parvocellular neurones of the PVN. THDOC significantly inhibited these neurones via a positive modulation of $GABA_A$ channels. Future studies will be necessary to investigate the effects of such hypothalamic neuroactive steroids on integration of the stress response, *in vivo*.

Acknowledgements

This work was funded by the British Heart Foundation.

Conflict of interest

The authors state no conflict of interest.

References

Akine A, Montanaro M, Allen AM (2003). Hypothalamic paraventricular nucleus inhibition decreases renal sympathetic nerve activity in hypertensive and normotensive rats. *Auton Neurosci* **108**: 17–21.

Badoer E (1996). Cardiovascular role of parvocellular neurons in the paraventricular nucleus of the hypothalamus. *News Physiol Sci* **11**: 43–47.

Barrett-Jolley R, Pyner S (2003). Inhibition of rat spinally projecting PVN neurones by the neurosteroid tetrahydroxycorticosterone. *J Physiol (London)* **548P**: P89.

Barrett-Jolley R, Pyner S, Coote JH (2000). Measurement of voltage-gated potassium currents in identified spinally-projecting sympathetic neurones of the paraventricular nucleus. *J Neurosci Methods* **102**: 25–33.

Bianchi MT, Macdonald RL (2001). Mutation of the 9′ leucine in the $GABA_A$ receptor [gamma]2L subunit produces an apparent decrease in desensitization by stabilizing open states without altering desensitized states. *Neuropharmacology* **41**: 737–744.

Black JW, Shankley NP (1985). The isolated stomach preparation of the mouse – a Physiological Unit for pharmacological analysis. *Br J Pharmacol* **86**: 571–579.

Buckingham JC (1996). Fifteenth Gaddum Memorial Lecture December 1994. Stress and the neuroendocrine–immune axis: the pivotal role of glucocorticoids and lipocortin 1. *Br J Pharmacol* **118**: 1–19.

Colquhoun D, Sakmann B (1985). Fast events in single-channel currents activated by acetylcholine and its analogs at the frog-muscle endplate. *J Physiol (London)* **369**: 501–557.

Connolly CN, Kittler JT, Thomas P, Uren JM, Brandon NJ, Smart TG *et al*. (1999). Cell surface stability of gamma-aminobutyric acid type A receptors – dependence on protein kinase C activity and subunit composition. *J Biol Chem* **274**: 36565–36572.

Cooper EJ, Johnston GAR, Edwards FA (1999). Effects of a naturally occurring neurosteroid on $GABA_A$ IPSCs during development in rat hippocampal or cerebellar slices. *J Physiol (London)* **521**: 437–449.

Coote JH (1995). Cardiovascular function of the paraventricular nucleus of the hypothalamus. *Biol Signal* **4**: 142–149.

Costantin JL, Charles AC (2001). Modulation of $Ca(2+)$ signaling by $K(+)$ channels in a hypothalamic neuronal cell line (GT1-1). *J Neurophysiol* **85**: 295–304.

Cui LN, Coderre E, Renaud LP (2001). Glutamate and GABA mediate suprachiasmatic nucleus inputs to spinal-projecting paraventricular neurons. *Am J Physiol Regul Integ Comp Physiol* **281**: R1283–R1289.

Duan YF, Winters R, Mccabe PM, Green EJ, Huang Y, Schneiderman N (1997). Cardiorespiratory components of defense reaction elicited from paraventricular nucleus. *Physiol Behav* **61**: 325–330.

Eghbali M, Curmi JP, Birnir B, Gage PW (1997). Hippocampal GABA(A) channel conductance increased by diazepam. *Nature* **388**: 71–75.

Fancsik A, Linn DM, Tasker JG (2000). Neurosteroid modulation of GABA IPSCs is phosphorylation dependent. *J Neurosci* **20**: 3067–3075.

Fenwick EM, Marty A, Neher E (1982). A patch-clamp study of bovine chromaffin cells and of their sensitivity to acetylcholine. *J Physiol (London)* **331**: 577–597.

Fischmeister R, Defelice LJ, Ayer Jr RK, Levi R, Dehaan RL (1984). Channel currents during spontaneous action potentials in embryonic chick heart cells. The action potential patch clamp. *Biophys J* **46**: 267–271.

Fritschy JM, Mohler H (1995). $GABA_A$-receptor heterogeneity in the adult rat brain: differential regional and cellular distribution of seven major subunits. *J Comp Neurol* **359**: 154–194.

Harrison NL, Majewska MD, Harrington JW, Barker JL (1987). Structure-activity relationships for steroid interaction with the gamma-aminobutyric acid A receptor complex. *J Pharmacol Exp Ther* **241**: 346–353.

Hosoya Y, Sugiura Y, Okado N, Loewy AD, Kohno K (1991). Descending input from the hypothalamic paraventricular nucleus to sympathetic preganglionic neurons in the rat. *Exp Brain Res* **85**: 10–20.

Li DP, Chen SR, Pan HL (2002). Nitric oxide inhibits spinally projecting paraventricular neurons through potentiation of presynaptic GABA release. *J Neurophysiol* **88**: 2664–2674.

Maitra R, Reynolds JN (1999). Subunit dependent modulation of $GABA_A$ receptor function by neuroactive steroids. *Brain Res* **819**: 75–82.

Majewska MD, Bisserbe JC, Eskay RL (1985). Glucocorticoids are modulators of $GABA_A$ receptors in brain. *Brain Res* **339**: 178–182.

Majewska MD, Harrison NL, Schwartz RD, Barker JL, Paul SM (1986). Steroid hormone metabolites are barbiturate-like modulators of the GABA receptor. *Science* **232**: 1004–1007.

Majewska MD, Mienville JM, Vicini S (1988). Neurosteroid pregnenolone sulfate antagonizes electrophysiological responses to GABA in neurons. *Neurosci Lett* **90**: 279–284.

Martin DS, Haywood JR (1993). Hemodynamic responses to paraventricular nucleus disinhibition with bicuculline in conscious rats. *Am J Physiol* **265**: H1727–H1733.

Martin DS, Segura T, Haywood JR (1991). Cardiovascular responses to bicuculline in the paraventricular nucleus of the rat. *Hypertension* **18**: 48–55.

Mienville JM, Vicini S (1989). Pregnenolone sulfate antagonizes $GABA_A$ receptor-mediated currents via a reduction of channel opening frequency. *Brain Res* **489**: 190–194.

Paul SM, Purdy RH (1992). Neuroactive steroids. *FASEB J* **6**: 2311–2322.

Paxinos G, Watson C (1986). *The Rat Brain in Stereotaxic Coordinates* 2nd edn. Academic Press: San Diego.

Purdy RH, Morrow AL, Moore Jr PH, PAUL SM (1991). Stress-induced elevations of gamma-aminobutyric acid type A receptor-active steroids in the rat brain. *Proc Natl Acad Sci USA* **88**: 4553–4557.

Pyner S, Coote JH (2000). Identification of branching paraventricular neurons of the hypothalamus that project to the rostroventrolateral medulla and spinal cord. *Neurosci* **100**: 549–556.

Reddy DS, Rogawski MA (2002). Stress-induced deoxycorticosterone-derived neurosteroids modulate GABA(A) receptor function and seizure susceptibility. *J Neurosci* **22**: 3795–3805.

Rho JH, Swanson LW (1989). A morphometric analysis of functionally defined subpopulations of neurons in the paraventricular nucleus of the rat with observations on the effects of colchicine. *J Neurosci* **9**: 1375–1388.

Sawchenko PE, Brown ER, Chan RK, Ericsson A, Li HY, Roland BL *et al*. (1996). The paraventricular nucleus of the hypothalamus and the functional neuroanatomy of visceromotor responses to stress. *Prog Brain Res* **107**: 201–222.

Schlenker E, Barnes L, Hansen S, Martin D (2001). Cardiorespiratory and metabolic responses to injection of bicuculline into the hypothalamic paraventricular nucleus (PVN) of conscious rats. *Brain Res* **895**: 33–40.

Shafton AD, Ryan A, Badoer E (1998). Neurons in the hypothalamic paraventricular nucleus send collaterals to the spinal cord and to the rostral ventrolateral medulla in the rat. *Brain Res* **801**: 239–243.

Sigworth FJ, Sine SM (1987). Data transformations for improved display and fitting of single-channel dwell time histograms. *Biophys J* **52**: 1047–1054.

Stotz-Potter EH, Morin SM, Dimicco JA (1996a). Effect of microinjection of muscimol into the dorsomedial or paraventricular hypothalamic nucleus on air stress-induced neuroendocrine and cardiovascular changes in rats. *Brain Res* **742**: 219–224.

Stotz-Potter EH, Willis LR, Dimicco JA (1996b). Muscimol acts in dorsomedial but not paraventricular hypothalamic nucleus to suppress cardiovascular effects of stress. *J Neurosci* **16**: 1173–1179.

Swanson LW, Kuypers HG (1980a). A direct projection from the ventromedial nucleus and retrochiasmatic area of the hypothalamus to the medulla and spinal cord of the rat. *Neurosci Lett* **17**: 307–312.

Swanson LW, Kuypers HG (1980b). The paraventricular nucleus of the hypothalamus: cytoarchitectonic subdivisions and organization of projections to the pituitary, dorsal vagal complex, and spinal cord as demonstrated by retrograde fluorescence double-labeling methods. *J Comp Neurol* **194**: 555–570.

Swanson LW, Sawchenko PE, Lind RW (1986). Regulation of multiple peptides in CRF parvocellular neurosecretory neurons: implications for the stress response. *Prog Brain Res* **68**: 169–190.

Wetzel CH, Vedder H, Holsboer F, Zieglgansberger W, Deisz RA (1999). Bidirectional effects of the neuroactive steroid tetrahydrodeoxycorticosterone on GABA-activated Cl^- currents in cultured rat hypothalamic neurons. *Br J Pharmacol* **127**: 863–868.

Zaki A, Barrett-Jolley R (2002). Rapid neuromodulation by cortisol in the rat paraventricular nucleus: an *in vitro* study. *Br J Pharmacol* **137**: 87–97.

Zhu WJ, Wang JF, Krueger KE, Vicini S (1996). Delta subunit inhibits neurosteroid modulation of $GABA_A$ receptors. *J Neurosci* **16**: 6648–6656.